The HIF-1α/miR-224-3p/ATG5 axis affects cell mobility and chemosensitivity by regulating hypoxia-induced protective autophagy in glioblastoma and astrocytoma

SIHUA HUANG[1], PENG QI[2], TING ZHANG[1], FENGTAO LI[1] and XIJING HE[1]

[1]Department of Orthopaedics, The Second Affiliated Hospital, School of Medicine, Xi'an Jiaotong University, Xi'an, Shaanxi 710000; [2]Department of Orthopaedics, Tangdu Hospital, Medical University of The Air Force, Xi'an, Shaanxi 710038, P.R. China

Received January 18, 2018; Accepted September 19, 2018

DOI: 10.3892/or.2018.6929

Abstract. Human glioblastoma is a malignant and aggressive primary human brain solid tumor characterized by severe hypoxia. Hypoxia can induce autophagy, which may result in chemoresistance and malignant progression of cancer cells. MicroRNAs (miRNAs) have been reported to modulate hypoxia-induced autophagy in various types of cancers. In the present study, we observed that hypoxia-inducible factor (HIF)-1α expression was increased while miR-224-3p expression was decreased under hypoxia in a time-dependent manner in glioma LN229 and astrocytoma U-251MG cell lines, as deteced by western blot analysis and real-time quantitative polymerase chain reaction. In addition, HIF-1α knockout inhibited cell motility and chemosensitivity by negatively regulating the expression of miR-224-3p under a hypoxic condition by Transwell and MTT assay. Moreover, hypoxia increased the relative expression of ATG5 (autophagy-related gene 5) and LC3 II/I with a decreased level of p62. These results were correlated with autophagy in a time-dependent manner, suggesting that hypoxia induced autophagy in glioblastoma and astrocytoma cells. Through bioinformatic prediction and luciferase reporter assay, we confirmed that ATG5 is a target of miR-224-3p and ATG5 expression was negatively regulated by miR-224-3p. Knockdown of ATG5 inhibited cell mobility with increased chemosensitivity of glioblastoma cells under hypoxia. Moreover, overexpression of miR-224-3p also inhibited cell mobility with increased chemosensitivity of glioblastoma cells under hypoxia. However, activation of autophagy was able to counteract these effects of miR-224-3p. Furthermore, *in vivo* experiments indicated that the miR-224-3p mimic enhanced the chemosensitivity of LN229 cells to temozolomide by immunohistochemistry and TUNEL assay. In summary, our experiments elucidated that the HIF-1α/miR-224-3p/ATG5 axis affects cell mobility and chemosensitivity by regulating hypoxia-induced autophagy in glioblastoma and astrocytoma. Therefore, miR-224-3p could be a novel target against hypoxia-induced autophagy in glioblastoma and astrocytoma.

Correspondence to: Dr Xijing He, Department of Orthopaedics, The Second Affiliated Hospital, School of Medicine, Xi'an Jiaotong University, 157 Xiwu Road, Xi'an, Shaanxi 710000, P.R. China
E-mail: hexijingsx@163.com

Abbreviations: HIF-1α, hypoxia-inducible factor α; miRNAs, microRNAs; ATG5, autophagy-related gene 5; TMZ, temozolomide; RT-qPCR; real-time quantitative polymerase chain reaction; SD, standard deviation; IC_{50}, half maximal inhibitory concentration

Key words: HIF-1α, miR-224-3p, ATG5, chemosensitivity, autophagy, glioblastoma

Introduction

Glioblastoma is the most malignant and aggressive primary human brain tumor of the central nervous system, with a high rate of recurrence and mortality (1). Although treatment including surgical resection combined with radiation and chemotherapy has been improved for glioblastoma therapy, the prognosis of glioblastoma patients is still very poor (2). Hypoxia is often observed in various types of solid tumors including glioblastoma, especially in the center of rapidly growing cancers with incomplete blood vessel networks (3). Hypoxia is considered as a main feature of the solid tumor microenvironment, playing an important role in tumor proliferation, metastasis and drug resistance (4). However, the molecular mechanism of how hypoxia regulates tumor progression in glioblastoma remains unknown and requires further research.

Hypoxia can induce the expression of hypoxia-inducible factor 1α (HIF-1α), which is an oxygen-dependent transcriptional activator (5). Activation of HIF-1α during hypoxia can regulate a great number of HIF target genes involved in cell proliferation, energy metabolism and angiogenesis (6,7). Autophagy, which is a mechanism of cellular degradation through lysosomes, is also involved in a HIF-1α-mediated cell survival mechanism (8,9). Hypoxia-induced autophagy can lead to chemoresistance and malignant progression of cancer cells (10). Therefore, suppression of hypoxia-induced autophagy may help inhibit the tumorigenesis of glioblastoma.

MicroRNAs (miRNAs) are a group of small non-coding RNAs with 17-22 nucleotides that regulate gene expression by blocking mRNA translation and/or mediating mRNA degradation (11). Under a hypoxic condition, a great number of miRNAs can regulate the expression of various autophagy-promoting genes and mediate autophagosome formation. For example, miR-101 was reported to be a potent inhibitor of autophagy and sensitize breast cancer cells to 4-hydroxytamoxifen (4-OHT)-mediated cell death (12). miR-130a was found to inhibit autophagy through targeting ATG2B and DICER1 and triggering the killing of chronic lymphocytic leukemia cells (13). However, it is still unclear whether or not miRNAs modulate hypoxia-induced autophagy in glioblastoma cells.

In the present study, we found that the relative expression of miR-224-3p was significantly downregulated in glioblastoma cells LN229 and astrocytoma cell line U-251MG under a hypoxic condition. Overexpression of miR-224-3p inhibited hypoxia-induced autophagy through the HIF-1α/miR-224-3p/ATG5 (autophagy-related gene 5) axis. Our study highlights the relationship among hypoxia, miRNAs and autophagy in glioblastoma and astrocytoma and aids in the identification of a novel miRNA against glioblastoma and astrocytoma progression.

Materials and methods

Cell culture and treatment. Human glioblastoma cell line LN229 and astrocytoma cell line U-251MG (Cell Bank, Shanghai Institutes for Biological Sciences, Shanghai, China) were cultured in Gibco™ Dulbecco's modified Eagle's medium (DMEM; Thermo Fisher Scientific, Inc., Waltham, MA, USA) supplemented with 10% FBS (HyClone, GE Healthcare Life Science, Logan, UT, USA) in a humidified atmosphere of 5% CO_2 at 37˚C. Hypoxia treatment was performed using a tri-gas incubator (37˚C, 5% CO_2, 93% N_2 and 2% O_2; YCP-50S, Changsha Huaxi Electronic Technology Co., Ltd., Hunan, China) for different periods (6, 12 and 24 h).

Temozolomide (TMZ) is an effective primary therapy for high-grade glioma. TMZ is a novel oral chemotherapy drug that penetrates into the brain and purportedly has a low incidence of adverse events (14). Stock solution of TMZ (Schering-Plough, Kenilworth, NJ, USA) was prepared by dissolving the drug in DMSO. TMZ was used to treat cells at different concentrations (0-80 μM). Rapamycin (Sigma-Aldrich; Merck KGaA, Darmstadt, Germany), an autophagy activator, was used to treat cells for 24 h at the concentration of 100 nM.

Western blot analysis. Cells were lysed in lysis buffer (Beyotime Institute of Biotechnolgy, Shanghai, China) and the concentrations of proteins were determined using a Pierce™ BCA protein assay kit (Thermo Fisher Scientific, Inc.). A total of 20 μg of protein was separated on 10% SDS-PAGE gel and then transferred into PVDF membranes (EMD Millipore, Billerica, MA, USA). After blocking with 5% BSA for 1 h at room temperature, the membranes were incubated with primary antibodies at 4˚C overnight. The following antibodies were used: anti-HIF-1α antibody (dilution 1:500; cat. no. ab51608; Abcam, Cambridge, UK), anti-ATG5 antibody (dilution 1:2,000; cat. no. ab108327; Abcam), anti-LC3 I/II antibody (dilution 1:1,000; cat. no. 12741; Cell Signaling Technology, Danvers, MA, USA), anti-p-62 antibody (dilution 1:1,000; cat. no. 88588; Cell Signaling Technology) and anti-GAPDH antibody (1:1,000; cat. no. 5174; Cell Signaling Technology). After incubation with horseradish peroxidase-conjugated secondary antibodies (dilution 1:2,000; cat. no. 7056; Cell Signaling Technology), the protein bands were detected by ImageJ software (version 1.48; National Institutes of Health, Bethesda, MD, USA).

Real-time quantitative polymerase chain reaction (RT-qPCR). Total RNA was extracted from the cells using TRIzol reagent (Takara Biotechnology Co., Ltd., Dalian, China). To detect mRNA expression of miR-224-3p, extracted RNA (1 μg) was reversely transcribed into cDNA using a miScript reverse transcription kit (Qiagen, Dusseldorf, Germany). Primer sequences were as follows: Forward 5'-TGATGTGGGTGC TGGTGTC-3' and reverse 5'-TTGTGTTGGGGCAGTACT G-3'; for ATG5: Forward 5'-GCCGAACCCTTTGCTCAA TG-3' and reverse 5'-TGGTCACCTTAGGAAATACCCAC-3'. SYBR Green Master Mix (Life Technologies; Thermo Fisher Scientific, Inc.) was used for gene expression level measurement. The expression levels were calculated using the ΔΔCq method (15) with U6 used for the normalization of miRNA.

Cell transfection. The siRNA against HIF-1α (HIF-1α siRNA), miR-224-3p mimic, siRNA against ATG5 (ATG5 siRNA) and the corresponding negative control (siRNA NC, mimic NC) were synthesized by Shanghai GenePharma Co. The sequences of HIF-1α-siRNAs were as follows: siRNA NC, 5'-UUCUCC GAACGUGUCACGUtt-3', HIF-1α siRNA1, 5'-UCACAGCAA UACAGAUUCAtt-3'; HIF-1α siRNA2, 5'-GCUCACCAU CAGUUAUUUAtt-3'; HIF-1α siRNA3, 5'-ACGCUCCUU GUCUUAUACCAtt-3'. The sequences of ATG5-siRNAs were as follows: siRNA NC, 5'-TATATGAAGAAAGTTATCTGG GTAT-3'; ATG5 siRNA1, 5'-ATTATTTAAAAATCTCTC ACTGTTG-3'; ATG5 siRNA2, 5'-TATAATATGAAGAAA GTTATCT GGTG-3'; ATG5 siRNA3, 5'-ATCTCACTGTTC ATTATCAAAGT-3'. Cells were seeded into 6-well plates and grown to reach 70% confluence for transfection. Transfection was performed with these molecular productions using Invitrogen™ Lipofectamine 2000 (Thermo Fisher Scientific, Inc.) according to the manufacturer's instructions.

Bioinformatic prediction and luciferase reporter assay. The targets of miR-224-3p were obtained from the following target prediction programs: PicTar (https://pictar.mdc-berlin .de/), miRDB (http://mirdb.org/miRDB/custom.html) and TargetScan (http://www.targetscan.org/vert_72/). The fragment of ATG5 containing the target sequence of miR-224-3p was amplified by RT-PCR and then inserted into a pmirGlO Dual-luciferase miRNA Target Expression Vector (Promega, Madison, WI, USA) to form the reporter vector ATG5-wild-type (ATG5-WT). Another expressing vector was also constructed by the insertion of a mutated binding site and was named as ATG5-mutated-type (ATG5-MUT). Cells were co-transfected with ATG5-WT or ATG5-MUT and miR-224-3p mimic respectively, and the Dual-Luciferase Reporter Assay system (Promega) was used for testing the luciferase activity.

Invasion assays. Invasion assays were analyzed using Transwell chambers coated with Matrigel (no. PIEP12R48, 8.0 μm; Millipore, USA). Cells ($1x10^5$ in 100 μl serum-free medium) were seeded into the top chamber and allowed to invade through the filter into the lower chamber containing medium with serum. After 24 h, cells on the top of the filter were removed while cells on the bottom were fixed in 4% paraformaldehyde. After that, the chambers were stained by crystal violet at 4˚C for 2 h. The cell numbers were counted and images were captured under an inverted microscope (Olympus Corp., Tokyo, Japan) at x400 magnification on 5 randomly selected fields in each well.

Wound healing assay. Cells ($5x10^5$) were seeded into 6-well plates and incubated for 24 h to reach 90-100% confluence. Then a sterile pipette tip (1-30 μl) was used to create a straight scratch to form a wound. After culturing for another 24 h, cells which migrated to the wounded area were visualized under a confocal microscope (Nikon A1; Nikon Corp., Tokyo, Japan; magnification, x200) at 0 and 24 h. Mitomycin C (10 μg/ml) was added to the cell culture medium to inhibit cell replication according to a previous report (16).

Cell viability assay. MTT assay was conducted to detect cell viability. Different groups of cells were seeded into 96-well plates at the concentration of $5x10^4$ cells/well. After incubating with different concentrations of temozolomide (TMZ) for 24 h, 20 μl of 5 mg/ml MTT solution (Sigma Chemicals; Merck KGaA) was added into the medium and incubated for 4 h at 37˚C in the dark. Then, the entire supernatant was replaced with 150 μl of dimethyl sulfoxide (DMSO; Sigma; Merck KGaA) to dissolve the formazan crystals for an additional 30 min at 37˚C. A microplate reader (Bio-Rad Laboratories, Inc., Hercules, CA, USA) was used to detect absorbance at 490 nm of each well.

Cell apoptosis assay. The cells ($2x10^5$ per well) were washed with phosphate-buffered saline (PBS) twice. Cell apoptosis was analyzed after appropriate plasmid transfection using staining with Annexin V and PI (BD Bioscience, San Jose, CA, USA) according to the manufacturer's instructions. After incubation for 15 min at room temperature in the dark, the cells were analyzed by using flow cytometry. Annexin V-positive and PI-negative/positive staining cells represented apoptotic cells.

In vivo animal study. All animal experiments were performed in accordance with the NIH Guide for the Care and Use of Laboratory Animals and were approved by the Medical Ethics Committee of Xi'an Jiaotong University. A total of 20 BALB/c nude mice (male, 4-weeks old) were obtained from the Animal Center of Xi'an Jiaotong University and housed in a controlled environment at 25±3˚C, humidity 60%, in a 12-h light/dark cycle with free access to food and water. LN229 cells ($2x10^5$) transfected with miR-224-3p mimic lentivirus (LV-miR-224-3p mimic) or negative control lentivirus (LV-mimic NC) or untreated LN229 cells were subcutaneously injected into the flank area of mice to form tumors. The mice were divided into 4 groups with 5 in each group: control group, mice injected with LN229 cells without TMZ treatment; TMZ group, mice injected with LN229 cells and received TMZ treatment by oral gavage (100 μM daily for 5 days per week for three cycles); TMZ+LV-mimic NC group, mice injected with LV-mimic NC transfected LN229 cells and received TMZ treatment; TMZ+LV-miR-224-3p mimic group, mice injected with LV-miR-224-3p mimic transfected LN229 cells and received TMZ treatment. Tumor volume and tumor weight were measured every 5 days post injection. Tumor volume (V) was calculated as follows: V (mm^3) = length x $width^2/2$. After 25 days post-injection, rats were euthanized by intraperitoneal injection of pentobarbital sodium (200 mg/kg body weight). Tumors were collected for the following experiments.

Immunohistochemistry. Immunohistochemical staining of nude mouse xenograft tumor tissues was performed with antibodies against VEGF (dilution 1:1,600; cat. no. 9698; Cell Signaling Technology) as previously described (17).

TUNEL assay. TUNEL assay was performed using Colorimetric TUNEL Apoptosis assay kit (Beyotime Institute of Biotechnology, Jiangsu, China) according to the manufacturer's instructions. Tumor sections were incubated with 3% H_2O_2 and then the TUNEL reaction mixture. The sections were rinsed and visualized using DAB. Hematoxylin was used for counter-staining. The numbers of TUNEL-positive cells from 6 random fields were counted under light microscopy Olympus Corp.) at x400 magnification. The cell apoptosis rate was calculated as the percent of TUNEL-positive cells relative to the total cells.

Statistical analysis. All experiments were performed in triplicate and the results in our present study are presented as mean ± standard deviation (SD). Statistical differences between experimental groups were analyzed with the SPSS version 20.0 (IBM Corp., Armonk, NY, USA) by utilizing one-way or two-way ANOVA followed by Bonferroni's post hoc test. A P-value <0.05 was considered to be statistically significant.

Results

Effect of hypoxia on the expression of HIF-1α and miR-224-3p. Firstly, we measured the expression of HIF-1α and miR-224-3p in LN229 and U-251MG cells under a hypoxic condition. The results showed that the expression of HIF-1α was increased in LN229 and U-251MG cells under hypoxia. The longer the duration of hypoxia, the higher the expression of HIF-1α (Fig. 1A and B, P<0.05 at 6 and 12 h, P<0.01 at 24 h). On the contrary, the expression of miR-224-3p was decreased under hypoxia condition in a time-dependent manner (Fig. 1C, P<0.05, P<0.01 at 12 and 24 h, respectively). Then, three different siRNA sequences were synthesized and transfected into LN229 and U-251MG cells. The highest knockout efficiency was detected by HIF-1α siRNA2 treatment in both LN229 and U-251MG cells (Fig. 1D, P<0.01). Thus, HIF-1α siRNA2 was selected for the following experiments. The transfection efficiency was further measured through western blot analysis (Fig. 1E, P<0.01). Moreover, we observed that knockdown of HIF-1α had no significant effect on the expression of miR-224-3p under a hypoxic condition (Fig. 1F). In addition,

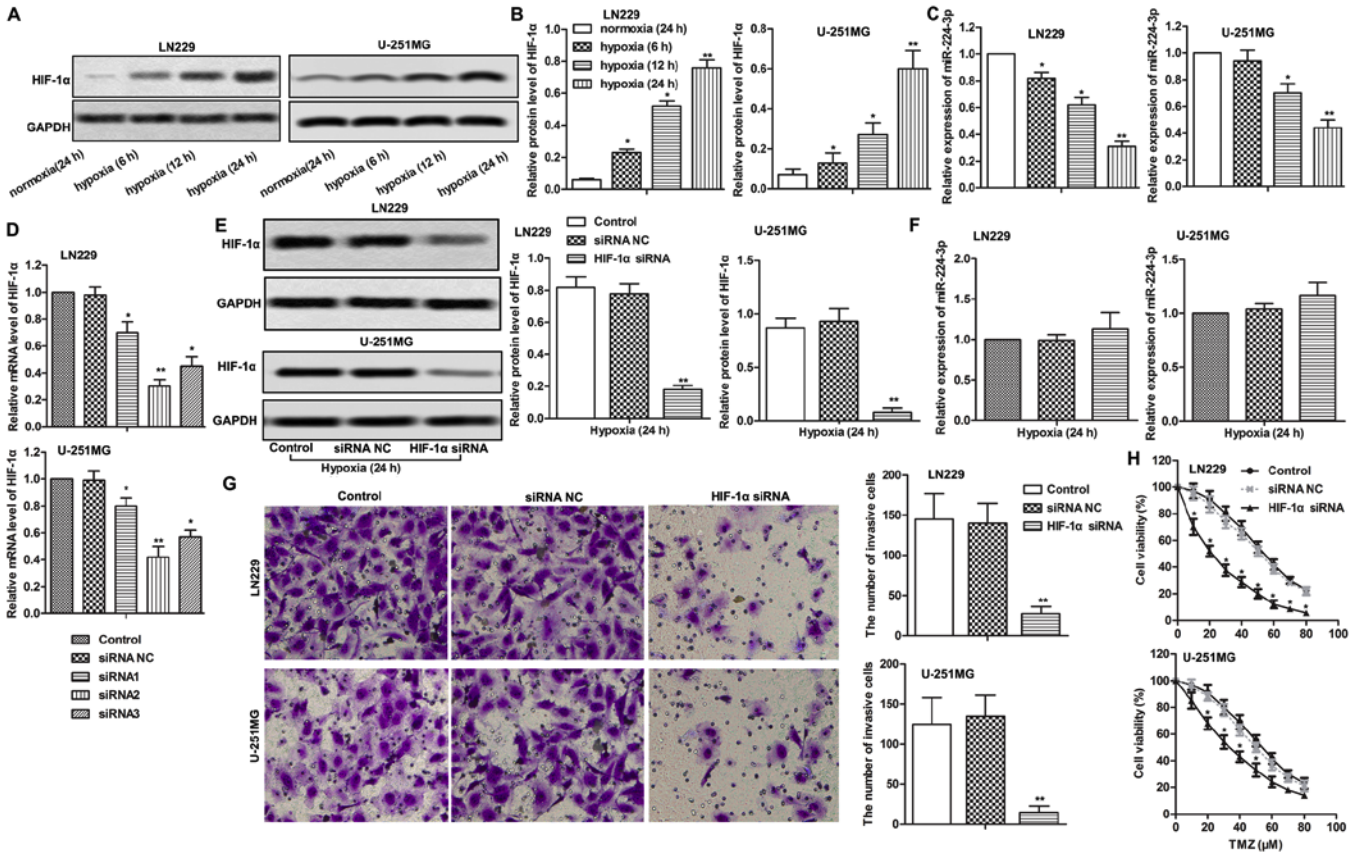

Figure 1. Effect of hypoxia on the expression of HIF-1α and miR-224-3p. (A) The expression level of HIF-1α in LN229 and U-251MG cells was detected by western blot analysis under a hypoxic condition for 6, 12 and 24 h. (B) Relative expression of HIF-1α in LN229 cells and U-251MG cells was analyzed and shown as a bar graph. (C) Relative level of miR-224-3p was detected by qRT-PCR in LN229 and U-251MG cells. *P<0.05, **P<0.01 compared with the normoxia group. (D) Three types of siRNAs specific for HIF-1α were transfected into LN229 and U-251MG cells, respectively. The mRNA expression level of HIF-1α was measured by qRT-PCR. (E) HIF-1α siRNA or siRNA NC transfected cells were cultured in a hypoxic condition. Relative expression of HIF-1α was detected through western blot analysis. (F) Relative expression of miR-224-3p was detected by qRT-PCR in LN229 and U-251MG cells. (G) The number of invasive LN229 and U-251MG cells was detected by Transwell assay. (H) The cell viability of LN229 and U-251MG cells was measured by MTT assay at different concentrations of TMZ. All data are represented as the mean ± SD from three independent experiments. *P<0.05, **P<0.01 vs. the control group.

the number of invasive cells was significantly decreased in the HIF-1α-knockout cells with increased chemosensitivity (Fig. 1G and H, P<0.05, P<0.01). These results indicated that HIF-1α influenced cell motility and chemosensitivity by negatively regulating the expression of miR-224-3p under a hypoxic condition.

Hypoxia induces autophagy in LN229 and U-251MG cells. Hypoxia was reported to induce autophagy of tumor cells. Here we detected the expression of autophagy-related proteins ATG5, LC3 I/II, p62 and found that the expression of these proteins in LN229 and U-251MG cells was significantly upregulated under hypoxia in a time-dependent manner. In addition, decreased level of autophagy substrate, p62, was observed in LN229 and U-251MG cells under hypoxia (Fig. 2A and B, P<0.05, P<0.01). Our data suggested that hypoxia induced autophagy in LN229 and U-251MG cells.

ATG5 is a target of miR-224-3p. Putative miR-224-3p targets were predicted through bioinformatic analysis and the results indicated that ATG5 was one of the potential targets of miR-224-3p (Fig. 3A). miR-224-3p mimic/inhibitor was transfected into LN229 cells to increase/decrease the expression of miR-224-3p (Fig. 3B, P<0.01). Overexpression of miR-224-3p significantly suppressed the expression of ATG5, while miR-224-3p inhibitor elevated the level of ATG5 (Fig. 3C and D, P<0.01). Results from the luciferase reporter assay showed that overexpression of miR-224-3p significantly inhibited luciferase activity in the wild-type ATG5 3'UTRs but not in the mutated 3'UTR plasmids (Fig. 3E, P<0.01), demonstrating the specificity of the miR-224-3p binding sites in 3'UTR of ATG5. These results demonstrated that ATG5 is a target of miR-224-3p.

ATG5 siRNA inhibits cell metastasis and increases chemosensitivity of LN229 cells under a hypoxic condition. To explore the regulating role of ATG5 in tumor progression of glioblastoma under hypoxia, three types of siRNAs were transfected into LN229 cells. ATG5 siRNA1 with the most effective inhibitory effect was selected to decrease the expression of ATG5 under a hypoxic condition (Fig. 4A and B, P<0.01). Knockdown of ATG5 inhibited cell invasion ability and migration ability of LN229 cells under hypoxia compared with the hypoxia (24 h)+siRNA NC group (Fig. 4C and D, P<0.01, P<0.001). In addition, the half maximal inhibitory concentration (IC_{50}) values of TMZ were approximately 20 and 50 μM in the hypoxia (24 h)+ATG5 siRNA group and hypoxia (24 h)+siRNA NC group, respectively, suggesting that

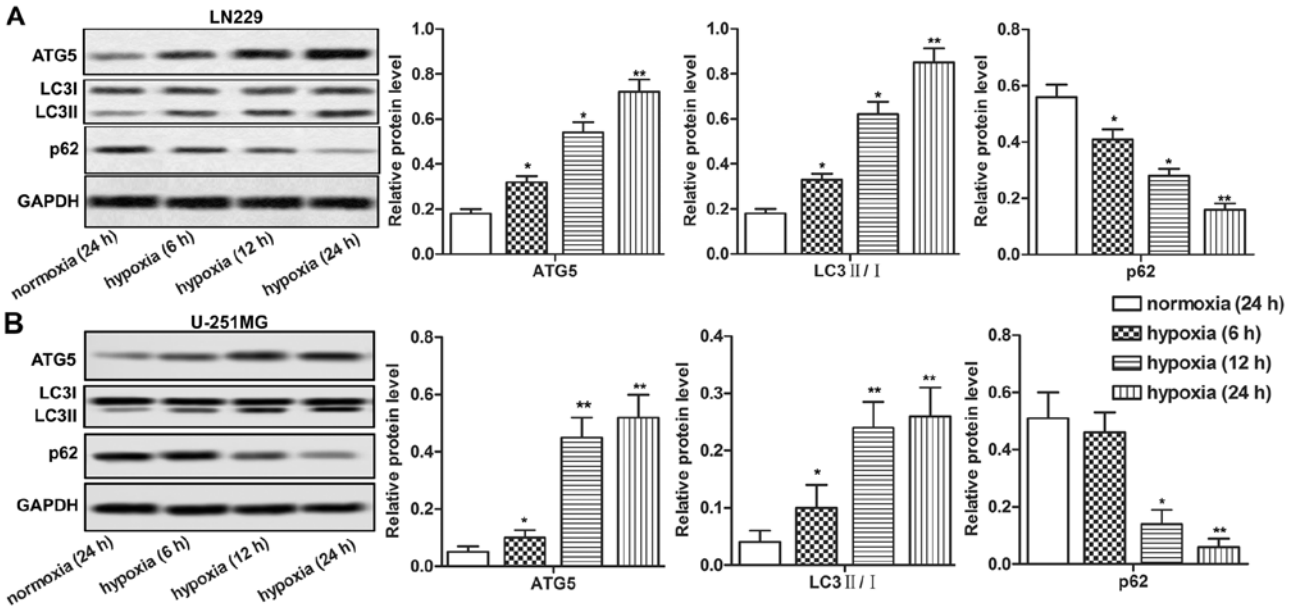

Figure 2. Hypoxia induced autophagy in LN229 and U-251MG cells. Cells were cultured in a normoxic or hypoxic condition for different times (6, 12, 24 h). (A) Relative expression of ATG5, LC3 I/II and p62 was detected through western blot analysis in LN229 cells. (B) Relative expression of ATG5, LC3 I/II and p62 was measured by western blot analysis in U-251MG cells. All data are represented as the mean ± SD from three independent experiments. *P<0.05, **P<0.01 compared with the normoxia group.

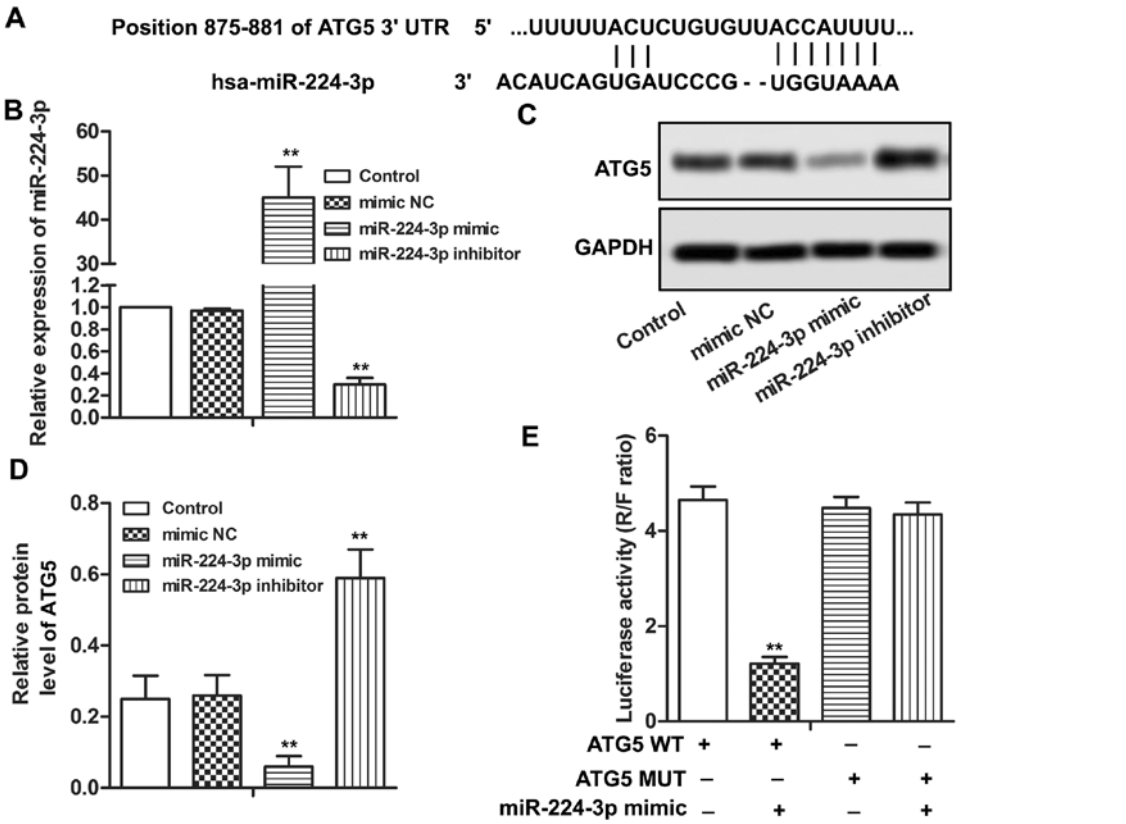

Figure 3. ATG5 is a target of miR-224-3p. LN229 cells were transfected with miR-224-3p mimic, inhibitor or mimic NC, respectively. (A) Target sequences of miR-224-3p in ATG5 mRNA were analyzed through bioinformatics. (B) Relative expression of miR-224-3p was detected through RT-qPCR. (C and D) Relative expression of ATG5 was detected through western blot analysis. **P<0.01 vs. the Control group. (E) The interaction between ATG5 and miR-224-3p was confirmed by luciferase reporter assay (**P<0.01 compared with the ATG5 WT group). All data are represented as the mean ± SD from three independent experiments.

ATG5 siRNA increased the chemosensitivity of LN229 cells under a hypoxic condition (Fig. 4E, P<0.05). Moreover, ATG5 siRNA increased cell apoptosis rates of TMZ-treated LN229 cells under a hypoxic condition (Fig. 4F, P<0.05). The above

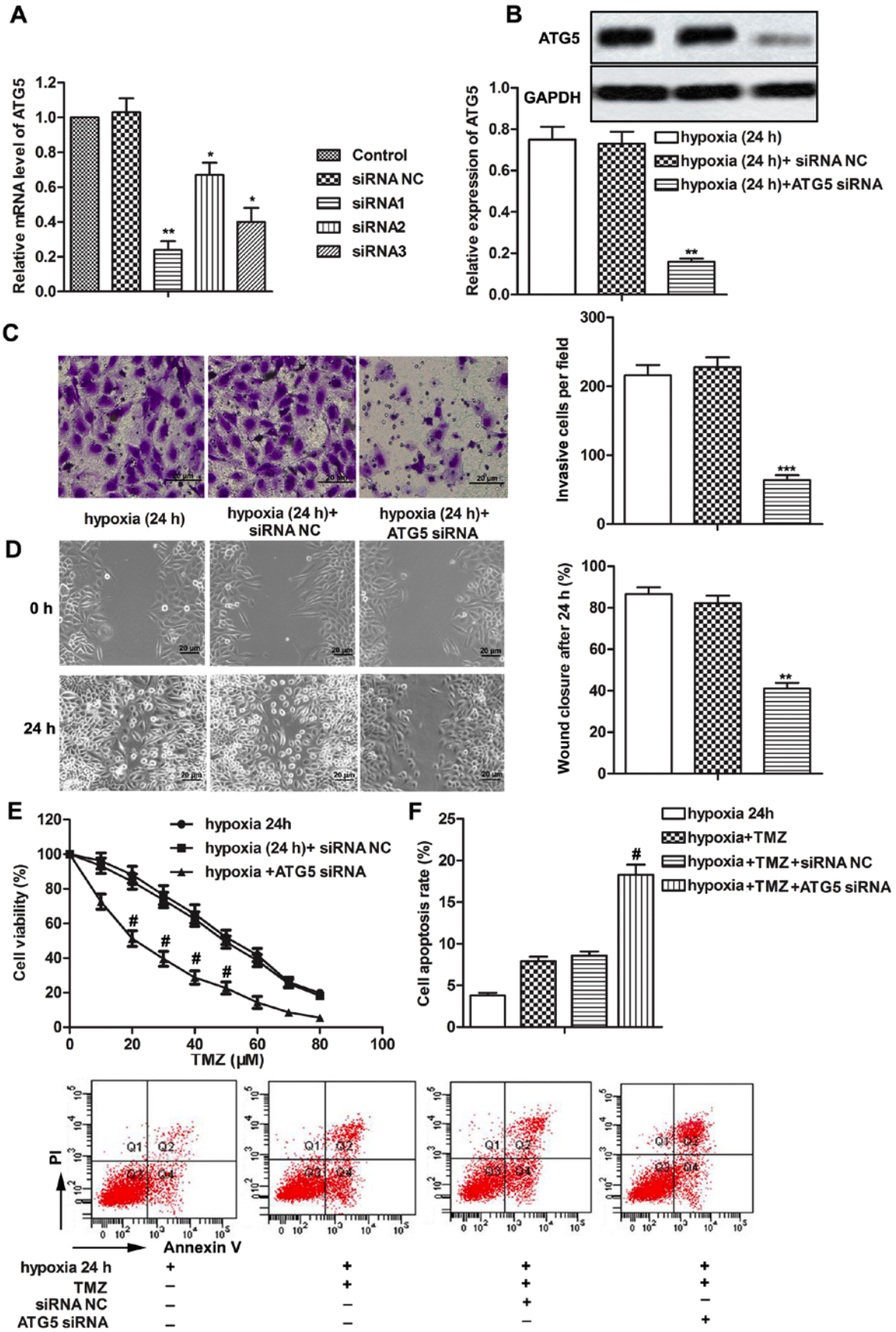

Figure 4. ATG5 siRNA inhibits cell metastasis and increases chemosensitivity of LN229 cells under a hypoxic condition. (A) Three types of siRNAs specific for ATG5 were transfected into LN229 cells. The mRNA expression level of ATG5 was measured by qRT-PCR. *P<0.05, **P<0.01 vs. the control group. (B) Relative expression of ATG5 was detected by western blot analysis. (C) The number of invasive cells was measured through Transwell assay. (D) Cell migration ability was measured through wound healing assay. (E) Cell viability was measured by MTT assay at different concentrations of TMZ. (F) Cell apoptosis rate was measured through flow cytometry analysis. All data are represented as the mean ± SD from three independent experiments. **P<0.01, ***P<0.001 compared with the hypoxia 24 h group; $^{\#}$P<0.05 compared with the hypoxia+TMZ+siRNA NC group.

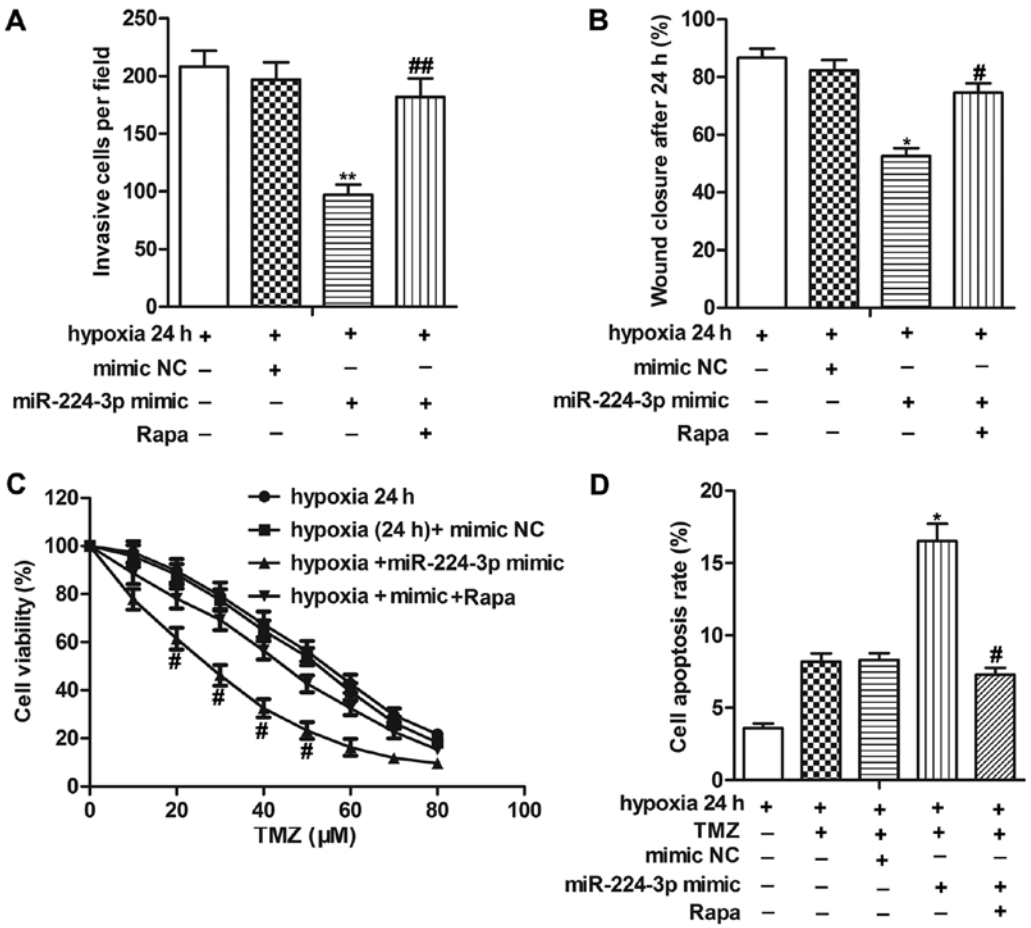

Figure 5. miR-224-3p mimic inhibits cell metastasis and increases chemosensitivity of LN229 cells under a hypoxic condition by suppressing autophagy. miR-224-3p mimic or mimic NC transfected LN229 cells were cultured in hypoxia condition for 24 h and received TMZ treatment with or without Rapa treatment. (A) Cell invasion ability was measured through Transwell assay. (B) Cell migration ability was measured through wound healing assay. (C) Cell viability was measured by MTT assay. (D) Cell apoptosis rate was measured through Hoechst 33258 staining analysis. All data are represented as the mean ± SD from three independent experiments. *P<0.05, **P<0.01 compared with the hypoxia 24 h+mimic NC group; $^{\#}$P<0.05, $^{\#\#}$P<0.01 compared with the hypoxia+miR-224-3p mimic group.

results indicated that ATG5 siRNA inhibited cell metastasis and increased chemosensitivity of LN229 cells under a hypoxic condition.

miR-224-3p mimic inhibits cell metastasis and increases chemosensitivity of LN229 cells under a hypoxic condition by suppressing autophagy. We then set to explore the role of miR-224-3p in tumor progression under hypoxia. Our data showed that the miR-224-3p mimic significantly suppressed the invasion and migration abilities of the LN229 cells under hypoxia. However, treatment with Rapa, an autophagy activator significantly counteracted the inhibitory role of the miR-224-3p mimic on cell metastasis of LN229 cells (Fig. 5A and B, P<0.01 for invasion; P<0.05, for wound closure). In addition, the IC_{50} values of TMZ were approximately 28 and 50 μM in the hypoxia (24 h)+miR-224-3p mimic group and hypoxia (24 h)+mimic NC group, respectively. miR-224-3p mimic increased the cell apoptosis rates of the TMZ-treated LN229 cells under hypoxia. The above results showed that miR-224-3p increased the chemosensitivity of LN229 cells under a hypoxic condition. However, Rapa treatment increased the IC_{50} values of TMZ while suppressing the cell apoptosis rate of the TMZ-treated LN229 cells under hypoxia compared with the hypoxia+miR-224-3p mimic group, indicating that activation of autophagy abolished the promoting role of miR-224-3p mimic on the chemosensitivity of LN229 cells under hypoxia (Fig. 5C and D, P<0.05, for both cell viability and apoptosis). These results elucidated that the miR-224-3p mimic inhibited cell metastasis and increased the chemosensitivity of LN229 cells under a hypoxic condition by suppressing autophagy.

miR-224-3p mimic enhances chemosensitivity of LN229 cells in vivo. A mouse xenograft model was constructed for our *in vivo* experiments. We found that tumor volume and tumor weight were both lower in the TMZ+LV-miR-224-3p mimic group compared with that in the TMZ+LV-mimic NC group, suggesting that the miR-224-3p mimic enhanced the chemosensitivity of LN229 cells to TMZ *in vivo* (Fig. 6A and B, P<0.05). Relative expression of HIF-1α and ATG5 were both down-regulated in the TMZ+LV-miR-224-3p mimic group compared with that noted in the TMZ+LV-mimic NC group (Fig. 6C, P<0.05). In addition, the miR-224-3p mimic suppressed the expression of VEGF with increased cell apoptosis rate compared with the TMZ+LV-mimic NC group (Fig. 6D and E, P<0.05). Taken together, our data indicated that

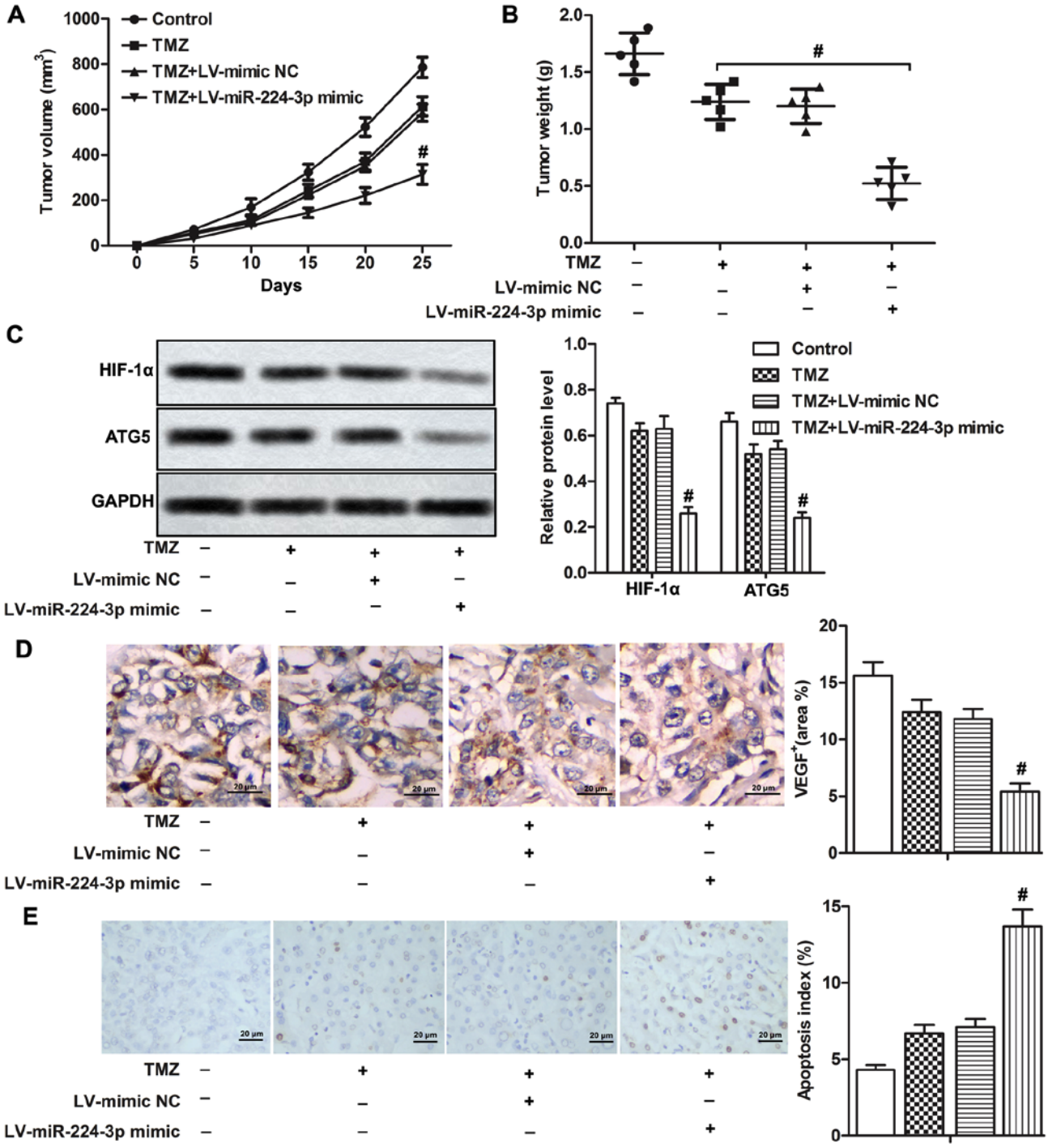

Figure 6. miR-224-3p mimic enhances the chemosensitivity of LN229 cells *in vivo*. LN229 cells transfected with miR-224-3p mimic lentivirus (LV-miR-224-3p mimic) or negative control lentivirus (LV-mimic NC) or untreated LN229 cells were subcutaneously injected into the flank area of mice to form tumors. TMZ was used to treat mice in these group apart from the control group. (A) Tumor volume was measured every 5 days. (B) Tumor weight was calculated. (C) Relative expression of HIF-1α and ATG5 was detected through western blot analysis. (D) Relative expression of VEGF was measured through immunohistochemistry (scale bar, 20 μm). (E) Apoptosis index was measured by TUNEL assay (scale bar, 20 μm). All data are represented as the mean ± SD from three independent experiments. $^{\#}$P<0.05 compared with the TMZ+LV-mimic NC group.

the HIF-1α/miR-224-3p/ATG5 axis regulated chemosensitivity of LN229 cells *in vivo*.

Discussion

Autophagy is a common cellular process that eliminates intracellular damaged organelles through the lysosomal pathway to sustain cell viability (18,19). Previous studies have reported that autophagy can induce resistance to radiotherapy or chemotherapy in various types of cancers, including breast, ovarian, head and neck cancers (20-23). Hypoxia, a well-known inducer of autophagy, is often observed in solid tumors due to inadequate blood supply, especially in rapid growing tumors such as glioblastoma (24,25). Recently, the regulating roles of miRNAs in hypoxia-induced autophagy have attracted attention. In our present study, we identified

hypoxia-mediated downregulation of miR-224-3p as a novel inhibitor of hypoxia-induced autophagy in glioblastoma and astrocytoma. The HIF-1α/miR-224-3p/ATG5 axis affected cell mobility and chemosensitivity in glioblastoma and astrocytoma by regulating hypoxia-induced autophagy both *in vitro* and *in vivo*.

Hypoxia induced the expression of HIF-1α, which plays a crucial role in various cellular processes during hypoxia. HIF-1α can induce cell cycle arrest (26), increase angiogenesis (27) and influence cell metabolism (28). Previous research reported that HIF-1α can regulate transcription of multiple miRNAs in hypoxia (29). The study by Silakit *et al* indicated that miR-210 acted as downstream of HIF-1α and was upregulated in various cancer cells under hypoxia condition (30). The research by Guo *et al* demonstrated that miR-224-3p was one of the downregulated miRNAs in glioblastoma cells under hypoxia (31). Similarly, in the present study, we found that the expression of HIF-1α was upregulated while the expression of miR-224-3p was downregulated under hypoxia in a time-dependent manner. Knockdown of HIF-1α significantly increased the expression of miR-224-3p, indicating that miR-224-3p acted as a downstream miRNA of HIF-1α under hypoxia. Moreover, we also demonstrated that hypoxia increased the relative expression of ATG5, LC3 II/I with decreased level of p62 which were correlated with autophagy in a time-dependent manner, suggesting that hypoxia induced autophagy in glioblastoma and astrocytoma cells. However, the role of the downregulation of miR-224-3p in hypoxia-induced autophagy warrants further investigation.

miRNAs can bind to their target genes and participate in multiple pathophysiologic processes by regulating their target gene expression (32). Through bioinformatic prediction and luciferase reporter assay, we confirmed that ATG5 was a target of miR-224-3p in our study. Overexpression of miR-224-3p significantly reduced the protein expression of ATG5, suggesting that the miR-224-3p mimic inhibits hypoxia-induced autophagy by suppressing ATG5 expression in glioblastoma.

ATG5 is a crucial molecular machinery component involved in autophagosome formation (33). Extensive research has demonstrated that ATG5 is a target of different miRNAs to adjust autophagy. For instance, miR-181a was reported to inhibit autophagy of cancer cells through targeting ATG5 (34). miR-216b was also found to attenuate autophagy in melanoma by targeting ATG5 (35). Moreover, upregulation of ATG5 was correlated with tumorigenesis of prostate cancer (36). In agreement with previous studies, we found that knockdown of ATG5 expression in transfected LN229 cells with ATG5 siRNA remarkably suppressed the invasive and migration abilities of LN229 cells under a hypoxic condition. In addition, knockdown of ATG5 increased the chemosensitivity of LN229 cells to TMZ and promoted cell apoptosis under TMZ treatment. These results demonstrated that knockdown of ATG5 suppressed cell mobility and chemoresistance of glioblastoma cells.

According to our results, knockdown of ATG5 suppressed cell mobility and chemoresistance of glioblastoma cells. The expression of ATG5 was inhibited by the miR-224-3p mimic; thus, we hypothesized that the miR-224-3p mimic inhibited cell mobility and chemoresistance of glioblastoma cells via suppressing ATG5-mediated autophagy under hypoxia. To verify our hypothesis, miR-224-3p was transfected into LN229 cells. Our data showed that overexpression of miR-224-3p inhibited cell mobility while increased chemosensitivity of glioblastoma cells under hypoxia. However, activation of autophagy was able to counteract these effects of miR-224-3p. In summary, our *in vitro* experiments elucidated that the HIF-1α/miR-224-3p/ATG5 axis affects cell mobility and chemosensitivity by regulating hypoxia-induced autophagy in glioblastoma cells.

Having elucidated the regulatory role of the HIF-1α/miR-224-3p/ATG5 axis in cell mobility and chemosensitivity *in vitro*, we then explored the effects of this axis using *in vivo* experiments. Previous research showed that overexpression of miR-224-3p suppressed tumor growth in a mouse xenograft model (31). Similarly, we observed that tumor volume and tumor weight were both smaller in the TMZ+LV-miR-224-3p mimic group, suggesting that the miR-224-3p mimic enhanced chemosensitivity of the LN229 cells to TMZ *in vivo*. In addition, the miR-224-3p mimic decreased HIF-1α, ATG5 and VEGF expression while promoting apoptosis of tumor cells under TMZ treatment, suggesting that the HIF-1α/miR-224-3p/ATG5 axis regulated chemosensitivity of LN229 cells *in vivo*.

Taken together, we identified miR-224-3p as a novel inhibitor of hypoxia-induced autophagy by directly targeting ATG5 in glioblastoma and astrocytoma cells. HIF-1α influenced cell motility and chemosensitivity by negatively regulating the expression of miR-224-3p under hypoxia. Additionally, overexpression of miR-224-3p inhibited cell mobility and chemoresistance of glioblastoma cells via suppressing ATG5 mediated autophagy under hypoxia. Therefore, miR-224-3p could be a novel target against hypoxia-induced autophagy in glioblastoma and astrocytoma.

Acknowledgements

The authors would like to thank the members of The Second Affiliated Hospital, School of Medicine, Xi'an Jiaotong University and Tangdu Hospital, Medical University of the Air Force, for providing technical support concerning the present study.

Funding

No funding was received.

Availability of data and materials

The datasets used and/or analyzed during the current study are available from the corresponding author on reasonable request.

Authors' contributions

SH interpreted the data regarding the autophagy assay and the cell viability analysis, collected and analyzed the data. PQ was involved in the western blot and RT-qPCR analysis. TZ and FL were involved in the cell transfection, the animal model establishment, immunohistochemistry and TUNEL assay. XH was responsible for conceiving, designing, drafting and revising the manuscript. All authors read and approved the final manuscript and agree to be accountable for all aspects of

the work in ensuring that questions related to the accuracy or integrity of any part of the work are appropriately investigated and resolved.

Ethics approval and consent to participate

All animal experiments were performed in accordance with the NIH Guide for the Care and Use of Laboratory Animals and were approved by the Medical Ethics Committee of Xi'an Jiaotong University. In addition, all experiments were conducted following institutional guidelines of Xi'an Jiaotong University (Xi'an, China).

Patient consent for publication

Not applicable.

Competing interests

The authors declare that they have no competing interests.

References

1. Stupp R, Mason WP, van den Bent MJ, Weller M, Fisher B, Taphoorn MJ, Belanger K, Brandes AA, Marosi C, Bogdahn U, *et al*: Radiotherapy plus concomitant and adjuvant temozolomide for glioblastoma. N Engl J Med 352: 987-996, 2005.
2. Omuro A and DeAngelis LM: Glioblastoma and other malignant gliomas: A clinical review. JAMA 310: 1842-1850, 2013.
3. Pouysségur J, Dayan F and Mazure NM: Hypoxia signalling in cancer and approaches to enforce tumour regression. Nature 441: 437-443, 2006.
4. Wilson WR and Hay MP: Targeting hypoxia in cancer therapy. Nat Rev Cancer 11: 393-410, 2011.
5. Masoud GN and Li W: HIF-1α pathway: Role, regulation and intervention for cancer therapy. Acta Pharm Sin B 5: 378-389, 2015.
6. Vallée A, Guillevin R and Vallée JN: Vasculogenesis and angiogenesis initiation under normoxic conditions through Wnt/β-catenin pathway in gliomas. Rev Neurosci 29: 71-91, 2018.
7. Shrivastava R, Singh V, Asif M, Negi MPS and Bhadauria S: Oncostatin M upregulates HIF-1α in breast tumor associated macrophages independent of intracellular oxygen concentration. Life Sci 194: 59-66, 2018.
8. Rodríguez ME, Catrinacio C, Ropolo A, Rivarola VA and Vaccaro MI: A novel HIF-1α/VMP1-autophagic pathway induces resistance to photodynamic therapy in colon cancer cells. Photochem Photobiol Sci 16: 1631-1642, 2017.
9. Sun Y, Xing X, Liu Q, Wang Z, Xin Y, Zhang P, Hu C and Liu Y: Hypoxia-induced autophagy reduces radiosensitivity by the HIF-1α/miR-210/Bcl-2 pathway in colon cancer cells. Int J Oncol 46: 750-756, 2015.
10. Yang X, Yin H, Zhang Y, Li X, Tong H, Zeng Y, Wang Q and He W: Hypoxia-induced autophagy promotes gemcitabine resistance in human bladder cancer cells through hypoxia-inducible factor 1α activation. Int J Oncol 53: 215-224, 2018.
11. Wang X, Ye X, Ji J, Wang J, Xu B, Zhang Q, Ming J and Liu X: MicroRNA155 targets myosin light chain kinase to inhibit the migration of human bone marrowderived mesenchymal stem cells. Int J Mol Med 42: 1585-1592, 2018.
12. Frankel LB, Wen J, Lees M, Høyer-Hansen M, Farkas T, Krogh A, Jäättelä M and Lund AH: microRNA-101 is a potent inhibitor of autophagy. EMBO J 30: 4628-4641, 2011.
13. Kovaleva V, Mora R, Park YJ, Plass C, Chiramel AI, Bartenschlager R, Döhner H, Stilgenbauer S, Pscherer A, Lichter P and Seiffert M: miRNA-130a targets ATG2B and DICER1 to inhibit autophagy and trigger killing of chronic lymphocytic leukemia cells. Cancer Res 72: 1763-1772, 2012.
14. Hart MG, Garside R, Rogers G, Stein K and Grant R: Temozolomide for high grade glioma. Cochrane Database Syst Rev: CD007415, 2013.
15. Livak KJ and Schmittgen TD: Analysis of relative gene expression data using real-time quantitative PCR and the 2(-Delta Delta C(T)) method. Methods 25: 402-408, 2001.
16. Milovic V, Teller IC, Murphy GM, Caspary WF and Stein J: Deoxycholic acid stimulates migration in colon cancer cells. Eur J Gastroenterol Hepatol 13: 945-949, 2001.
17. Wang YY, Sun G, Luo H, Wang XF, Lan FM, Yue X, Fu LS, Pu PY, Kang CS, Liu N and You YP: MiR-21 modulates hTERT through a STAT3-dependent manner on glioblastoma cell growth. CNS Neurosci Ther 18: 722-728, 2012.
18. Kroemer G, Mariño G and Levine B: Autophagy and the integrated stress response. Mol Cell 40: 280-293, 2010.
19. Nakatogawa H, Suzuki K, Kamada Y and Ohsumi Y: Dynamics and diversity in autophagy mechanisms: Lessons from yeast. Nat Rev Mol Cell Biol 10: 458-467, 2009.
20. He WS, Dai XF, Jin M, Liu CW and Rent JH: Hypoxia-induced autophagy confers resistance of breast cancer cells to ionizing radiation. Oncol Res 20: 251-258, 2012.
21. Apel A, Herr I, Schwarz H, Rodemann HP and Mayer A: Blocked autophagy sensitizes resistant carcinoma cells to radiation therapy. Cancer Res 68: 1485-1494, 2008.
22. Wang J and Wu GS: Role of autophagy in cisplatin resistance in ovarian cancer cells. J Biol Chem 289: 17163-17173, 2014.
23. Sannigrahi MK, Singh V, Sharma R, Panda NK and Khullar M: Role of autophagy in head and neck cancer and therapeutic resistance. Oral Dis 21: 283-291, 2015.
24. Klionsky DJ and Emr SD: Autophagy as a regulated pathway of cellular degradation. Science 290: 1717-1721, 2000.
25. Höckel M and Vaupel P: Tumor hypoxia: Definitions and current clinical, biologic, and molecular aspects. J Natl Cancer Inst 93: 266-276, 2001.
26. Koshiji M, Kageyama Y, Pete EA, Horikawa I, Barrett JC and Huang LE: HIF-1alpha induces cell cycle arrest by functionally counteracting Myc. EMBO J 23: 1949-1956, 2004.
27. Clara CA, Marie SK, de Almeida JR, Wakamatsu A, Oba-Shinjo SM, Uno M, Neville M and Rosemberg S: Angiogenesis and expression of PDGF-C, VEGF, CD105 and HIF-1α in human glioblastoma. Neuropathology 34: 343-352, 2014.
28. Agani F and Jiang BH: Oxygen-independent regulation of HIF-1: Novel involvement of PI3K/AKT/mTOR pathway in cancer. Curr Cancer Drug Targets 13: 245-251, 2013.
29. Kulshreshtha R, Ferracin M, Negrini M, Calin GA, Davuluri RV and Ivan M: Regulation of microRNA expression: The hypoxic component. Cell Cycle 6: 1426-1431, 2007.
30. Silakit R, Kitirat Y, Thongchot S, Loilome W, Techasen A, Ungarreevittaya P, Khuntikeo N, Yongvanit P, Yang JH, Kim NH, *et al*: Potential role of HIF-1-responsive microRNA210/HIF3 axis on gemcitabine resistance in cholangiocarcinoma cells. PLoS One 13: e0199827, 2018.
31. Guo X, Xue H, Guo X, Gao X, Xu S, Yan S, Han X, Li T, Shen J and Li G: MiR224-3p inhibits hypoxia-induced autophagy by targeting autophagy-related genes in human glioblastoma cells. Oncotarget 6: 41620-41637, 2015.
32. Jafarzadeh M, Mohammad Soltani B, Ekhteraei Tousi S and Behmanesh M: Hsa-miR-497 as a new regulator in TGFβ signaling pathway and cardiac differentiation process. Gene 675: 150-156, 2018.
33. Mallik A and Yammani RR: Saturated fatty acid palmitate negatively regulates autophagy by promoting ATG5 protein degradation in meniscus cells. Biochem Biophys Res Commun 502: 370-374, 2018.
34. Tekirdag KA, Korkmaz G, Ozturk DG, Agami R and Gozuacik D: MIR181A regulates starvation- and rapamycin-induced autophagy through targeting of ATG5. Autophagy 9: 374-385, 2013.
35. Luo M, Wu L, Zhang K, Wang H, Wu S, O'Connell D, Gao T, Zhong H and Yang Y: miR-216b enhances the efficacy of vemurafenib by targeting Beclin-1, UVRAG and ATG5 in melanoma. Cell Signal 42: 30-43, 2017.
36. Li X, Li C and Zhu LH: Correlation of autophagy-associated gene Atg5 with tumorigenesis of prostate cancer. Zhonghua Nan Ke Xue 21: 31-34, 2015 (In Chinese).